Distinguishing NFW and Isothermal Density Profiles with Weak Gravitational Lensing

Ian Holst and Doyee Byun

May 8, 2018

Abstract

We examine the feasibility of distinguishing NFW and cored isothermal density profiles using weak gravitational lensing shear.

We model lenses in the two different profiles, as well as background galaxies to be lensed. Analyzing the simulated data of these lensed galaxies gives us insight into how we can distinguish the differences between the two profiles. This method is expected to be helpful in the analysis of real observation data in the future.

1 Introduction

Gravitational lensing allows us to investigate the matter density distributions of cosmic objects by observing the characteristic distortions imparted on other objects in the background. The principle is applicable on a large range of scales, from all-sky mass maps based on cosmic microwave background shear to studies of individual galaxies and clusters. In particular, by observing the coherent distortions of many background galaxies, the shear profile, and consequently the density profile of a foreground halo lens may be determined.

Two commonly used density profiles in the field are the isothermal profile and the Navarro-Frenk-White (NFW) profile. The NFW profile has been found to fit simulated dark matter halos very well [], while the isothermal profile . Both profiles have infinite extent

Lensing offers one of the only ways to probe the distribution In this paper, we will investigate the distinguishability of given galaxy-galaxy lensing data

We start with introducing the general characteristics of spherical density profiles, followed by cored isothermal and NFW profiles. We then describe the purpose of our project, to distinguish between NFW and isothermal profiles, in detail. The goal of this project is to devise a method to analyze lensed galaxy cluster data and find which density profile is more probable between the isothermal and NFW profiles. In order to do so, we generate simulated data sets and analyze them to find the more probable profiles they would fit into. This analysis method is expected to be usable in determining the characteristics of real observed data as well.

Estimating ellipticity has well-documented issues [cite] due to noise and PSF

We describe the common characteristics of spherical density profiles. Here we define our conventions for various lensing quantities, which mainly conform to those used by Dodelson [2017]. We use the thin lens approximation and assume spherical lens profiles. Consider such a spherically symmetric halo density profile $\rho(r)$

The lens halo is located at an angular diameter distance D_L from the observer and we want to consider its effects on a source object behind it at an angular diameter distance D_S.

The projected surface density at radius R on the projected plane is defined, considering the z axis to be along the line of sight:

$$\Sigma(R) = \int_{-\infty}^{\infty} dz\ \rho(\sqrt{R^2 + z^2}) \tag{1}$$

An important related measure in gravitational lensing is the average projected surface density within radius R:

$$\overline{\Sigma}(R) = \frac{1}{\pi R^2} \int_0^{2\pi} d\phi \int_0^R dR'\ \Sigma(R')R' \tag{2}$$

The critical surface density marks the typical boundary between what is considered strong and weak lensing:

$$\Sigma_{\text{crit}} = \frac{c^2}{4\pi G} \frac{D_S}{(D_S - D_L)D_L} \tag{3}$$

At small angles, we can assume from small angle approximations that $R = D_L\theta$.

We also define the convergence, κ to be

$$\kappa(\theta) = \frac{\Sigma(\theta)}{\Sigma_{\text{crit}}} \tag{4}$$

Strong lensing features take over when the convergence is greater than one. Tangential shear, along with the components of shear are shown as follows.

$$\gamma_t(\theta) = \overline{\kappa}(\theta) - \kappa(\theta) \tag{5}$$

The tangential shear is decomposed into two components, γ_1 and γ_2. γ_1 represents stretching along the θ_x and θ_y axes, and γ_2

$$\begin{aligned} \gamma_1 &= -\gamma_t \cos 2\phi \\ \gamma_2 &= -\gamma_t \sin 2\phi \end{aligned} \tag{6}$$

It can be shown that for a spherical lens profile, the only component of shear γ should be the tangential shear, γ_t: [Dodelson, 2017]

$$\gamma = \gamma_t = \sqrt{{\gamma_1}^2 + {\gamma_2}^2} = -\gamma_1 \cos 2\phi - \gamma_2 \sin 2\phi \tag{7}$$

Deflection angle is

$$\vec{\alpha}(\vec{\theta}) = \overline{\kappa}(\theta)\vec{\theta} \tag{8}$$

$$\vec{\beta} = \vec{\theta} - \vec{\alpha} = (1 - \overline{\kappa}(\theta))\vec{\theta} \tag{9}$$

while ellipticity is

$$\epsilon_i = \frac{2\gamma_i/(1-\kappa)}{1 + \gamma^2/(1-\kappa)^2} \tag{10}$$

$$\epsilon = -\epsilon_1 \cos 2\phi - \epsilon_2 \sin 2\phi \tag{11}$$

2 Cored Isothermal Sphere Profile

The cored isothermal sphere (CIS) profile is related to the singular isothermal sphere profile, which is often used to describe halos and other collapsed astrophysical objects because of its simple formulation. Unlike the singular isothermal sphere, the cored isothermal sphere does not have a density singularity at its center due to a finite core radius r_c. The CIS density profile is defined:

$$\rho_{\rm iso}(r) = \frac{\sigma^2}{2\pi G(r^2 + {r_c}^2)} \tag{12}$$

where σ^2 is the velocity dispersion. https://arxiv.org/pdf/astro-ph/9810164.pdf

$$\Sigma_{\rm iso}(\theta) = \frac{\sigma^2}{2GD_L\sqrt{\theta^2 + {\theta_c}^2}} \tag{13}$$

$$\overline{\Sigma}_{\rm iso}(\theta) = \frac{\sigma^2\left(\sqrt{\theta^2 + {\theta_c}^2} - \theta_c\right)}{GD_L\theta^2} \tag{14}$$

$$\gamma_{\rm iso}(\theta) = \frac{\sigma^2\left(\sqrt{\theta^2 + {\theta_c}^2} - \theta_c\right)}{\Sigma_{\rm crit}GD_L\theta^2} - \frac{\sigma^2}{2\Sigma_{\rm crit}GD_L\sqrt{\theta^2 + {\theta_c}^2}} \tag{15}$$

We switch dependence from σ^2 to M_{200} with:

$$\sigma^2 = \frac{M_{200}G}{2\left(r_{200} - r_c\arctan\left(\frac{r_{200}}{r_c}\right)\right)} \tag{16}$$

This is derived from the definition of M_{200}:

$$M_{200} = 200\rho_{\rm crit}\frac{4}{3}\pi {r_{200}}^3 \tag{17}$$

$$M_{200} = M_{\rm enc}(r_{200}) = \frac{2\sigma^2}{G}\left(r_{200} - r_c\arctan\left(\frac{r_{200}}{r_c}\right)\right) \tag{18}$$

$$r_{200} = \left(\frac{3M_{200}}{800\pi\rho_{\rm crit}}\right)^{1/3} \tag{19}$$

The ellipticity equations, while not quite elegant, are trivial to calculate from the shear.

3 Navarro-Frenk-White (NFW) Profile

$$\rho_{\rm NFW}(r) = \frac{\rho_{\rm crit}\delta_c}{(r/r_s)\left(1 + r/r_s\right)^2} \tag{20}$$

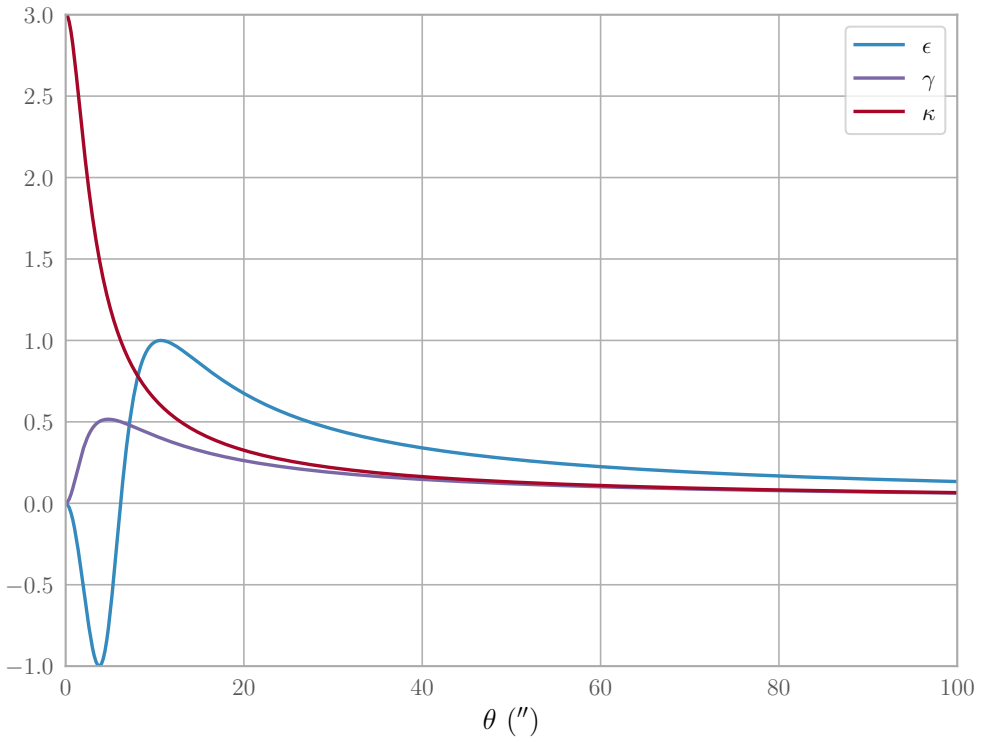

Figure 1: Lensing quantities for a CIS profile with $M_{200} = 10^{15} M_\odot$ and $r_c = 10$ kpc.

$$\Sigma_{\rm NFW}(\theta) = \frac{2\rho_{\rm crit}\delta_c D_L \theta_s}{(\theta/\theta_s)^2 - 1}\left(1 - \frac{2}{\sqrt{(\theta/\theta_s)^2 - 1}}\arctan\left(\sqrt{\frac{\theta/\theta_s - 1}{\theta/\theta_s + 1}}\right)\right) \tag{21}$$

$$\overline{\Sigma}_{\rm NFW}(\theta) = \frac{4\rho_{\rm crit}\delta_c D_L \theta_s}{(\theta/\theta_s)^2}\left(\frac{2}{\sqrt{(\theta/\theta_s)^2 - 1}}\ \arctan\left(\sqrt{\frac{\theta/\theta_s - 1}{\theta/\theta_s + 1}}\right) + \ln\left(\frac{\theta/\theta_s}{2}\right)\right) \tag{22}$$

Similar convention used by Bartelmann et al. [2001]

$$\gamma_{\rm NFW}(\theta) = \frac{\overline{\Sigma}_{\rm NFW}(\theta) - \Sigma_{\rm NFW}(\theta)}{\Sigma_{\rm crit}} \tag{23}$$

We can calculate ellipticities from tangential shear.

We switch the dependence to M_{200} and c with:

$$\delta_c = \frac{200}{3}\frac{c^3}{\ln(1+c) - c/(1+c)} \tag{24}$$

$$r_s = \frac{r_{200}}{c} \tag{25}$$

$$r_{200} = \left(\frac{3M_{200}}{800\pi\rho_{\rm crit}}\right)^{1/3} \tag{26}$$

$$c = \frac{r_{200}}{r_s} \tag{27}$$

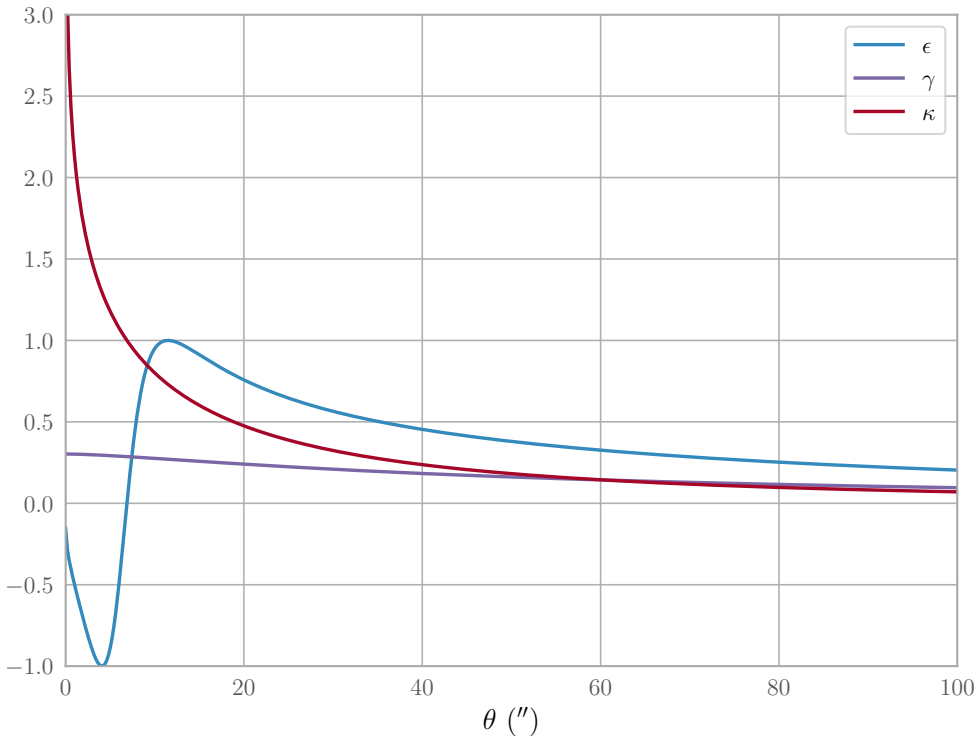

Figure 2: Lensing quantities for a NFW profile with $M_{200} = 10^{15} M_\odot$ and $c = 10$.

4 Methods

4.1 Modelling of Foreground Lens and Background Galaxies

Based on the calculations shown above, we have modelled singular lenses corresponding to each density profile. Background galaxies have been generated via randomization of angular coordinates.

1. Consider single foreground lens halo with many background galaxies.
    - Start with one NFW halo, then maybe consider more tests.
2. Construct background galaxies:
    - Number density on sky: 50 galaxies/square arcminute (LSST, https://arxiv.org/pdf/1305.0793.pdf)
    - Intrinsic ellipticity drawn from Gaussian distribution with $\mu = 0, \sigma = 0.2$ (consistent with https://arxiv.org/pdf/1509.05058.pdf)
    - Assume they are all that the same distance D_S since this can be determined by redshift (neglecting some noise)
    - Apply shear and deflection angles to background galaxies to get simulated data: N sets of ϵ_1, ϵ_2, θ_1, θ_2
3. Recommended values:

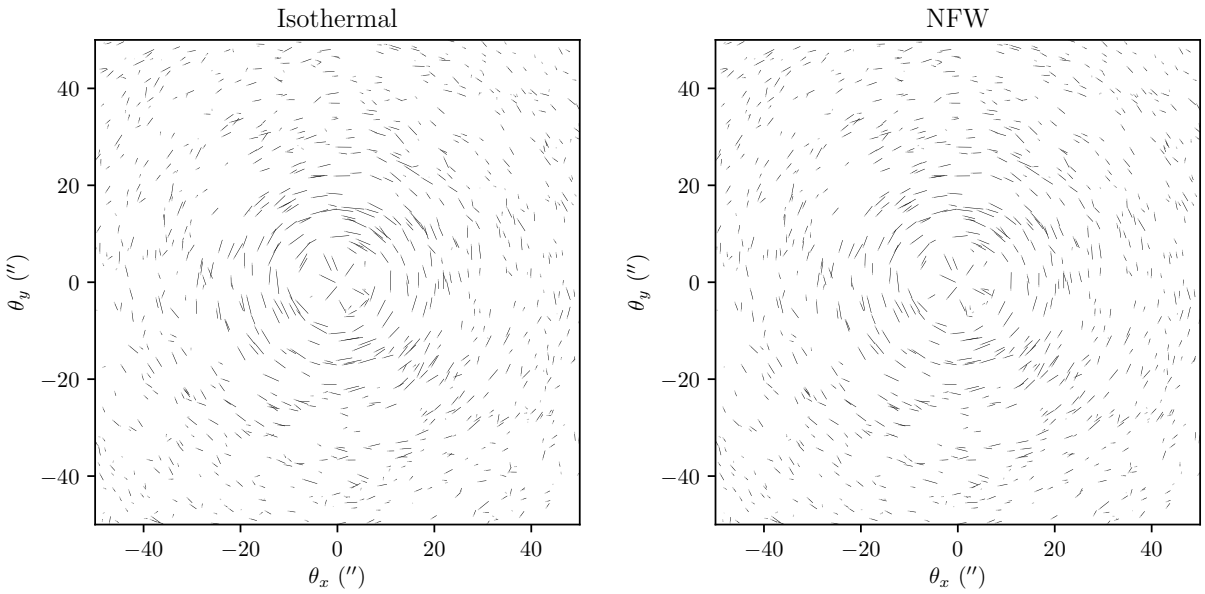

Figure 3: plots

- $z_L = 0.3$ (bullet cluster)
- $z_S = 1.0$ (Hubble Deep Field) (also consistent with https://arxiv.org/pdf/1509.05058.pdf) we use the planck 2015 results
- $M_{halo} = 10^{15} M_\odot$

4.2 Data Analysis and Density Profile Determination

1. Bin galaxies in annuli by θ value (use log bins for theta)
2. Calculate mean and standard deviation of ellipticity
3. Attempt to fit both NFW and isothermal profiles, see if the fit is distinguishable

5 Results

6 Conclusions

Like (COMPARISONS BETWEEN ISOTHERMAL AND NFW MASS PROFILES FOR STRONG-LENSING GALAXY CLUSTERS), we find that the strong lensing regime provides the most But also, weak lensing can in fact provide sufficient distinguishability

has been applied to observations before https://arxiv.org/pdf/astro-ph/9602053.pdf but not in the context of comparing density profiles using for strong and weak but this is highly dependent on good data

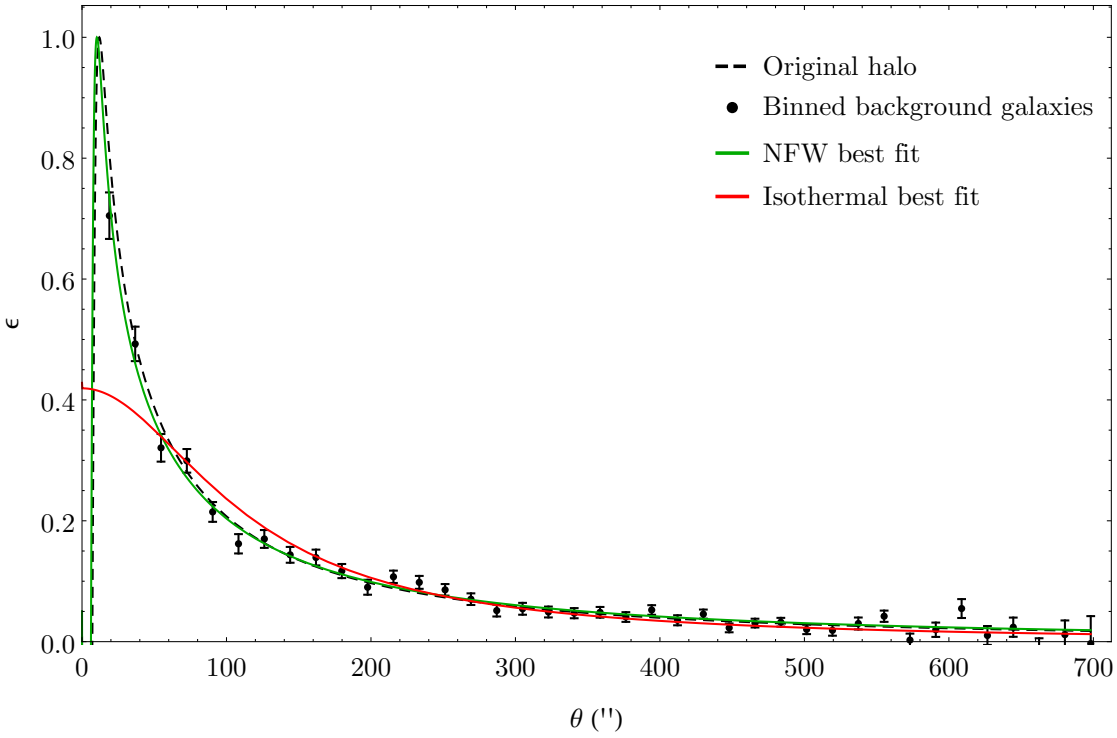

Figure 4: plots

http://iopscience.iop.org/article/10.1086/590049/pdf looked at NFW vs isothermal in strong lensing with a focus on arcs, and found differing levels of distinguishibility for different lenses.

https://arxiv.org/pdf/1101.0650.pdf - our results don't match

ignore cosmic shear (https://journals.aps.org/prd/pdf/10.1103/PhysRevD.70.023008)

From our data analysis, we were able to find the more probable density profile of a simulated data set. Since the simulated data is based on the NFW and isothermal profile models, we were able to decisively distinguish between the two. When analyzing real observed data, we expect the probability ratios to be relatively more even. Future goals include the use of these methods to analyze observed data of galaxy clusters to find the density profile of their lenses.

References

M. Bartelmann, L. J. King, and P. Schneider. Weak-lensing halo numbers and dark-matter profiles. *A&A*, 378(2):361–369, nov 2001. ISSN 0004-6361. doi: 10.1051/0004-6361:20011199. URL `http://www.edpsciences.org/10.1051/0004-6361:20011199`.

S Dodelson. *Gravitational Lensing*. Cambridge University Press, jun 2017.